Steady-state thermodynamics: Description equivalence and violation of reservoir independence

Leonardo Ferreira Calazans ©[*] and Ronald Dickman ©[†]

Departamento de Física and National Institute of Science and Technology for Complex Systems, ICEx, Universidade Federal de Minas Gerais, C. P. 702, 30123-970 Belo Horizonte, Minas Gerais, Brazil

For stochastic lattice models in spatially uniform nonequilibrium steady states, an *effective* thermodynamic temperature T and chemical potential μ can be defined via coexistence with heat and particle reservoirs. We verify that the probability distribution P_N for the number of particles in the driven lattice gas with nearest-neighbor exclusion in contact with a particle reservoir with dimensionless chemical potential μ^* possesses a large-deviation form in the thermodynamic limit. This implies that the thermodynamic properties determined in isolation (fixed particle number representation) and in contact with a particle reservoir (fixed dimensionless chemical potential representation) are equal. We refer to this as *description equivalence*. This finding motivates investigation of whether the effective intensive parameters so obtained depend on the nature of the exchange between system and reservoir. For example, a stochastic particle reservoir is usually taken to insert or remove a single particle in each exchange, but one may also consider a reservoir that inserts or removes a pair of particles in each event. In equilibrium, equivalence of pair and single-particle reservoirs is guaranteed by the canonical form of the probability distribution on configuration space. Remarkably, this equivalence is violated in nonequilibrium steady states, limiting the generality of steady-state thermodynamics based on intensive variables.

I. INTRODUCTION

Despite progress on many fronts, extending thermodynamics to far-from-equilibrium systems remains an unsolved challenge. An attractive preliminary goal is a thermodynamic description of nonequilibrium steady states (NESS), that is, steady-state thermodynamics [1,2]. By thermodynamics, we understand a macroscopic description using a small number of variables, having predictive power. A fundamental question is the prediction of coexistence: Consider two systems, $\mathcal{S}_A$ and $\mathcal{S}_B$ in NESS, that are weakly coupled via exchange of energy and/or particles. What values will macroscopic quantities assume when the systems reach coexistence, i.e., a stationary state, such that the net mean fluxes between the two systems vanish? One approach to predicting properties at coexistence involves defining effective intensive parameters in NESS [3–5] such that coexisting systems possess identical values of the relevant intensive parameters, just as in equilibrium thermodynamics. Recently, an approach to defining effective intensive parameters via coexistence with stochastic reservoirs has achieved a measure of success (including a zeroth law of thermodynamics) when applied to spatially uniform systems, provided the exchange rates satisfy two conditions: detailed balance and a factorization property [2,3,5–7]. For such systems, this definition allows one to predict coexistence properties.

This achievement motivates further investigations exploring the consequences of this definition of intensive parameters. In Ref. [8], the authors defined an entropy function via nonequilibirum thermodynamic integration of effective intensive parameters and found that it is different from the Shannon entropy, and is not a state function. In Refs. [9,10], it was shown that this definition is not able to predict densities of nonuniform systems (e.g., for a nonequilibrium drive applied to half the system or to a driven system confined between walls). Moreover, this definition does not allow prediction of phase coexistence in models such as the Katz-Lebowitz-Spohn (KLS)-driven lattice gas [11]. These violations can be understood as a consequence of nonfactorizing exchange rates between two regions, as shown by Guioth and Bertin [4]. A number of works explore definitions of intensive parameters via large-deviation analysis [4–6] or a nonequilibrium free energy for NESS [12]. These studies conclude that under some conditions, such as the additivity of the large-deviation function and a macroscopic detailed balance condition, it is possible to define intensive parameters for NESS.

In this paper, we investigate the equivalence of thermodynamic approaches. A fundamental property of equilibrium thermodynamics is the equivalence of the descriptions associated with distinct representations. Thus, one can choose among entropy, Helmholtz, Gibbs, and other representations according to convenience. The entropy, Helmholtz and grand-potential representations, describe, respectively, the system in isolation (microcanonical ensemble), in contact with an (energy) reservoir (canonical ensemble), and in contact with an energy and a particle reservoir (grand canonical ensemble). In equilibrium statistical mechanics, the various ensembles treat a system in contact (or not) with reservoirs of distinct quantities, and ensemble equivalence includes the possibility of treating a small subsystem $\mathcal{S}'$ of a large isolated system $\mathcal{S}$ as if it were in contact with a reservoir formed by the complement

*leonardo.ferreira.calazans@gmail.com
†dickman@fisica.ufmg.br

of $\mathcal{S}'$ in $\mathcal{S}$. In NESS, full ensemble equivalence, extending to subsystems, is, in general, ruled out due to the fluxes that characterize nonequilibrium, but we may still inquire as to the equivalence of representations in which a NESS is in contact with an external reservoir or is isolated. We call this property *description equivalence*.

We briefly review basic notions regarding a system $\mathcal{S}$ in contact with a stochastic reservoir $\mathcal{R}$. A reservoir $\mathcal{R}$ is a system much larger than $\mathcal{S}$ such that exchanges between them do not alter the value of the intensive parameter(s). We regard $\mathcal{R}$ as a system that attempts to exchange particles and/or energy with any system $\mathcal{S}$ with which it is placed in contact. The attempt rates governing this exchange are independent of $\mathcal{S}$, in particular, of whether $\mathcal{S}$ is in equilibrium or not. (The fraction of attempted exchanges that are accepted does, of course, depend on the state of $\mathcal{S}$.) Suppose the internal dynamics of $\mathcal{S}$ allows it to attain equilibrium. In this case, $\mathcal{S}$ attains equilibrium with $\mathcal{R}$ when the two are placed in contact, implying that the exchange rates must satisfy detailed balance relations consistent with the intensive properties (temperature and chemical potential) of the reservoir. Equilibrium between $\mathcal{S}$ and $\mathcal{R}$ occurs when their intensive properties are equal, and is independent of the *manner* in which exchange occurs.

Now consider a system $\mathcal{S}$ in a NESS. When placed in contact with a reservoir, it may attain a state of *zero net flux* with $\mathcal{R}$, i.e., a new NESS. We call this situation *coexistence* between $\mathcal{S}$ and $\mathcal{R}$ to avoid confusion with equilibrium between $\mathcal{S}$ and $\mathcal{R}$. As mentioned above, coexistence with a stochastic reservoir associates an effective intensive parameter or parameters with $\mathcal{S}$. In fact, under certain restrictions, two systems $\mathcal{S}_1$ and $\mathcal{S}_2$ (either or both of which are in NESS) coexist under direct exchange if both coexist with the same reservoir, yielding a zeroth law of thermodynamics for effective intensive parameters [3]. Further, effective intensive parameters of a NESS *not in contact* with a reservoir can be defined using the idea of *virtual exchange* [3].

The foregoing observations raise two questions as we attempt to extend the formalism of equilibrium statistical thermodynamics to NESS:

(i) Are the descriptions of (a) a NESS in coexistence with a reservoir and (b) a NESS free of such contact, equivalent in the infinite-size limit?

(ii) Do the values of the effective intensive parameters associated with a NESS depend on the *manner* of exchange with $\mathcal{R}$?

In this paper, we examine these issues in the context of the NNE lattice gas, a system of *interacting* particles that can be maintained *far* from equilibrium in a NESS. We provide an affirmative answer to the first question, based on numerical evidence for the existence of a large-deviation function. We also show that, unlike in equilibrium, the values of the effective intensive parameter(s) characterizing a NESS do, in fact, depend on the manner in which exchange with $\mathcal{R}$ is realized. This restricts the generality of effective intensive parameters, compared with equilibrium.

For NESS, no general principle is known for determining the stationary probability distribution on configuration space; it must instead be found by solving the master equation. This stationary solution generally has a detailed dependence

on the transition rates, including those describing exchanges between $\mathcal{S}$ and $\mathcal{R}$. One can nevertheless ask if the physical descriptions in both frameworks ($\mathcal{S}$ in contact with $\mathcal{R}$ or not) are equivalent in the thermodynamic limit (TL). We consider three levels of equivalence. First, macroscopic equivalence, which means that the values of stationary means of macroscopic quantities of interest are equal in both frameworks in the TL. The second is thermodynamic equivalence, i.e., thermodynamic properties of a system in isolation determined from measuring the effective chemical potential as a function of density are the same as thermodynamic properties of a system in contact with a particle reservoir with the density determined by the chemical potential of $\mathcal{R}$. Finally, the third level is measure equivalence, which means that the probability densities associated with the two descriptions are equal in the TL [13].

Construction of descriptions for NESS depends on defining effective intensive parameters. Bertin and coauthors [6] explore the definition of ensembles for the zero-range process [14], a model with a factorizable stationary probability distribution, which is far from a general situation for NESS. Recently, a more general formulation of the grand canonical ensemble, based on large-deviation theory was proposed by Guioth and Bertin [15].

The driven NNE lattice gas is a simple model with nontrivial properties such as an order-disorder phase transition. In isolation, the model is characterized by three parameters: particle number N, system size V, and drive strength D. For the fixed-N description, the dimensionless effective chemical potential $\mu^* \equiv \mu/k_{\mathrm{B}}T$ can be evaluated via virtual contact; assuming that one particle can be inserted or removed in each virtual exchange event, this parameter is given by [3]

$$\mu^* = \ln \frac{\rho}{\tilde{\rho}_{\mathrm{op}}}, \qquad (1.1)$$

where $\tilde{\rho}_{\mathrm{op}}$ is the mean density of open sites in the stationary state with fixed particle number, N. When $\mathcal{S}$ is in contact with particle reservoir, N fluctuates; let the stationary probability distribution be $\tilde{P}_N$. The condition of coexistence between $\mathcal{S}$ and $\mathcal{R}$ under weak contact implies

$$\mu^* = \ln \frac{\langle \rho \rangle}{\langle \tilde{\rho}_{\mathrm{op}} \rangle}, \qquad (1.2)$$

where $\langle \cdot \rangle$ denotes the stationary mean with respect to $\tilde{P}_N$.

Although expressions (1.1) and (1.2) are superficially similar, the quantities involved are associated with distinct stochastic processes, so that equivalence of the two expressions for μ^* is not immediately evident.

The remainder of this paper is organized as follows. In Sec. II, we define the NNE model used in our investigation. In Sec. III, we discuss coexistence of a NESS with a particle reservoir and present results on description equivalence, based on numerical evidence for a large-deviation function. We discuss reservoir independence (or lack thereof) in Sec. IV, followed, in Sec. V, by our conclusions and comments on avenues for further investigation.
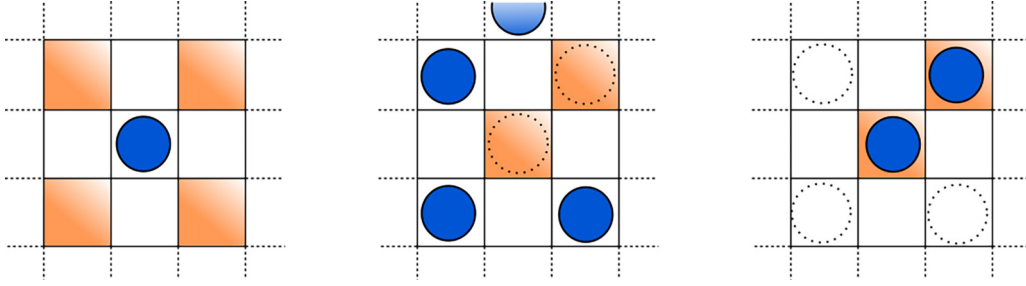
FIG. 1. In the left panel, a particle occupies the central site. White sites: first-nearest neighbors; colored sites: second neighbors. Center panel: The two colored sites represent a pair of open second-neighbors. Right panel: The colored sites highlight a pair of particles occupying second-neighbor sites.

II. DRIVEN LATTICE GAS WITH NEAREST-NEIGHBOR EXCLUSION MODEL

We study a driven lattice gas with nearest-neighbor exclusion (NNE) on square lattices of $L \times L$ sites with periodic boundaries. Each site of the lattice can be occupied by at most one particle; occupancy of a site implies that its four nearest neighbors (NNs) be vacant. A configuration $\mathcal{C}$ consists of N particles distributed over the lattice, obeying the NNE condition; in equilibrium, all N-particle configurations are equally probable. The configuration evolves according to a continuous-time (i.e., sequential) Markovian dynamics of particle jumps. Each particle can hop to a first or second neighbor if the resulting configuration satisfies the NNE conditions. Consider a transition from configuration $\mathcal{C}$ to $\mathcal{C}'$, generated by displacing particle j by $\boldsymbol{\ell} = (\Delta x, \Delta y)$, where Δx and Δy can assume values in the set $\{-1, 0, 1\}$ (excluding, of course, $\Delta x = \Delta y = 0$). The transition rate from $\mathcal{C}$ to $\mathcal{C}'$, denoted by $w(\mathcal{C}'|\mathcal{C})$, depends on the direction of the jump: letting $\mathbf{D} = D\mathbf{i}$, $w(\mathcal{C}'|\mathcal{C}) = \epsilon(1 + \mathbf{D} \cdot \boldsymbol{\ell}) = \epsilon(1 + D\Delta x)$, where ϵ is a constant with dimensions $1/(\text{time})$, and $D \in [-1, 1]$. Thus, jumps with $\boldsymbol{\ell} \cdot \mathbf{D} > 0 (< 0)$ are favored (inhibited), while jumps perpendicular to the drive $\mathbf{D}$ are not affected by it. $D = 0$ corresponds to equilibrium, while for $D \neq 0$ the system is maintained out of equilibrium, leading to a particle current in the steady state. The dynamics conserves the total number of particles N [16].

The probability distribution over N-particle configurations, $p_{\mathcal{C}|N}(t)$, satisfies the master equation,

$$\frac{dp_{\mathcal{C}|N}(t)}{dt} = \sum_{\mathcal{C}' \in \Gamma(L,N)} [w(\mathcal{C}|\mathcal{C}')p_{\mathcal{C}|N}(t) - w(\mathcal{C}'|\mathcal{C})p_{\mathcal{C}|N}(t)],$$

(2.1)

where $\Gamma(L, N)$ denotes the set of all N-particle configurations on a lattice of size L. In the stationary state, $dp_{\mathcal{C}|N}/dt = 0 \,\forall\, \mathcal{C}$, we denote the stationary probability distribution with a fixed number of particles by $\tilde{p}_{\mathcal{C}|N}$ [20].

In the NNE lattice gas, since interactions are due to excluded volume only, all configurations have the same energy and the system is athermal, characterized (in equilibrium) by a single independent intensive parameter. In the fixed-N description, the natural choice for this parameter is the density $\rho = N/L^d$. When we consider a NNE lattice gas ($\mathcal{S}$) in coexistence with a particle reservoir $\mathcal{R}$, it is the effective dimensionless chemical potential, μ^* (a property of $\mathcal{R}$) that is

fixed, while N, of course, fluctuates. In the familiar case in which $\mathcal{S}$ and $\mathcal{R}$ exchange a single particle in each transfer, the properties of $\mathcal{R}$ discussed in Sec. I imply that the ratio of the insertion and removal *attempt* rates be $\exp[\mu^*]$. In the fixed-μ^* description, the density is given by $\rho(\mu^*) = \langle N \rangle / L$, which is a nondecreasing function of μ^*. We note that, since the NNE lattice gas is athermal and the particles do not possess momenta, there is no need for defining a temperature. Following the usual custom, one may nevertheless write $\mu^* \equiv \mu/k_B T$, where μ is the effective chemical potential, T is a temperature, and k_B is Boltzmann's constant.

The fixed-N description *also* permits definition of an effective dimensionless chemical potential $\mu^*(\rho)$: it is the value associated with a reservoir $\mathcal{R}$ that *would coexist with $\mathcal{S}$, were particle exchange allowed*. The resulting relation, Eq. (1.1), for virtual exchange between $\mathcal{S}$ and $\mathcal{R}$, is familiar from Widom's particle insertion method [21]. In this case, μ^* is a nondecreasing function of the density ρ.

In the presence of a nonzero drive D, the NESS is governed by two independent intensive parameters: ρ and D in the fixed-N description, and μ^* and D when the system coexists with a particle reservoir. Thus $\mu^* = \mu^*(\rho, D)$ in the fixed-N case, while $\rho = \rho(\mu^*, D)$ in the fixed-μ^* description.

In addition to the density, $\rho = N/L^2$, several other configurational properties are relevant to our discussion. The number of *open sites*, $N_{op}(\mathcal{C})$, in configuration $\mathcal{C}$ is the number of sites at which a particle can be inserted without violating the NNE condition. The number of doubly occupied second-neighbor pairs of sites is $N^{(2)}(\mathcal{C})$, and the doubly open second-neighbor pairs of sites is $N_{op}^{(2)}(\mathcal{C})$, with associated densities $\rho_{op} = N_{op}(\mathcal{C})/L^2$, $\rho_d = N^{(2)}(\mathcal{C})/(2L^2)$, and $\rho_{op}^{(2)} = N_{op}^{(2)}(\mathcal{C})/(2L^2)$. (See Fig. 1 for examples.) Figure 2 shows estimates of these densities obtained via Monte Carlo simulation for $L = 160$ and $D = 1$.

Given L, the number of possible densities is $1 + L^2/2$. For instance, when $L = 56$ the number of densities is 1569, implying a huge number of studies if one were to analyze each case individually. Nevertheless, since ρ_{op}, $\rho^{(2)}$, and $\rho_{op}^{(2)}$ are smooth functions of density in the infinite-size limit, one can perform simulations for representative values of ρ in the interval $(0, 1/2)$, and fit a polynomial to these data to estimate the properties at intermediate values. In this paper, we use data for $L = 10$, 20, 28, 56, 64, 96, 128, 160. For $L \geqslant 56$, we study 30 values of the density. The absolute errors associated
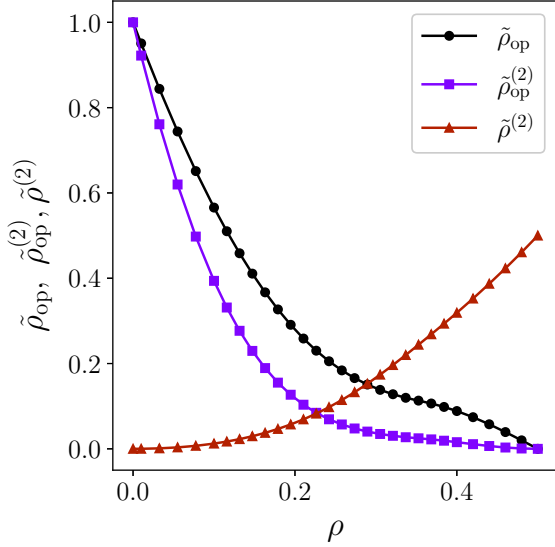
FIG. 2. Stationary mean of the open-site density $\tilde{\rho}_{\text{op}}$ (black circles) and densities of pairs of open second neighbors $\tilde{\rho}_{\text{op}}^{(2)}$ (blue squares), and doubly occupied of second neighbors $\tilde{\rho}^{(2)}$ (red triangles), obtained via Monte Carlo simulation for $L = 160$ and $D = 1$. Error bars are smaller than symbols.

with interpolation are $\sim 10^{-5}$, an order of magnitude smaller than the statistical uncertainties of the simulations.

III. COEXISTENCE, EFFECTIVE INTENSIVE PARAMETERS AND RESERVOIRS

Our definition of the dimensionless chemical potential μ^* is based on coexistence: We say that systems $\mathcal{S}$ and $\mathcal{S}'$, in steady states (in or out of equilibrium), have the same value of μ^* if and only if they coexist under exchange of particles. Temperature and other intensive parameters can be defined in the same manner for systems that can exchange energy, or other quantities [3].

If one of the coexisting systems is much larger than the other, we can regard it as a particle reservoir $\mathcal{R}_\zeta$, characterized only by its value of μ^* and its manner ζ of exchanging particles. An exchange scheme ζ involves all details of exchange dynamics including rates, the set of sites (boundaries, bulk, etc.) through which exchange occurs, and the number of particles (ΔN_ζ) exchanged in each event. In accord with the above definition, any system $\mathcal{S}$ that coexists with reservoir $\mathcal{R}$ has the same effective chemical potential, $\mu_\mathcal{S}^* = \mu_\mathcal{R}^*$. The rates of insertion and removal satisfy detailed balance with respect to the stationary probability distribution, as discussed in Sec. I. Let $\mathcal{C}$ denote a configuration with N particles, and $\mathcal{C}'$ a configuration resulting from inserting ΔN_ζ particles in $\mathcal{C}$. Further, let $w(\mathcal{C}'|\mathcal{C}) \equiv w_{\text{ins}}(\mathcal{R}_\zeta)$ denote the particle insertion attempt rate under contact with $\mathcal{R}_\zeta$, and $w(\mathcal{C}|\mathcal{C}') \equiv w_{\text{rem}}(\mathcal{R})$ the corresponding removal attempt rate. Then detailed balance requires

$$\frac{w(\mathcal{C}'|\mathcal{C})}{w(\mathcal{C}|\mathcal{C}')} = \frac{w_{\text{ins}}(\mathcal{R}_\zeta)}{w_{\text{rem}}(\mathcal{R}_\zeta)} = e^{\Delta N_\zeta \mu^*}. \quad (3.1)$$

In an exchange attempt, $\mathcal{R}_\zeta$ randomly selects sites in $\mathcal{S}$ according to the restrictions (if any) specified in ζ. The number

of possible sets that the reservoir can select is denoted $\mathcal{N}_\zeta$. (For example, if $\Delta N_\zeta = 1$, and exchange can occur at *any site* in $\mathcal{S}$, then $\mathcal{N}_\zeta = L^2$, the number of sites.) Thus, we choose the insertion rate as $w_{\text{ins}}(\mathcal{R}_\zeta) = \epsilon e^{\Delta N_\zeta \mu^*}/\mathcal{N}_\zeta$, and the removal rate as $w_{\text{rem}}(\mathcal{R}_\zeta) = \epsilon/\mathcal{N}_\zeta$, with $1/\mathcal{N}_\zeta$ denoting the probability of selecting a specific set of sites.

The particle current between system and reservoir is given by

$$J_N^\zeta(\mu^*; \{\tilde{p}_\mathcal{C}\}) = \Delta N_\zeta \sum_\mathcal{C} \left[w_{\text{ins}}(\mathcal{R}_\zeta) \Pi_{\text{ins}}^\zeta(\mathcal{C}) \tilde{p}_\mathcal{C} \right.$$
$$\left. - w_{\text{rem}}(\mathcal{R}_\zeta) \Pi_{\text{rem}}^\zeta(\mathcal{C}) \tilde{p}_\mathcal{C} \right], \quad (3.2)$$

where $\Pi_{\text{ins}}^\zeta(\mathcal{C})$ ($\Pi_{\text{rem}}^\zeta(\mathcal{C})$) is the number of insertion (removal) transitions possible from $\mathcal{C}$. Note that $\Pi_{\text{ins}}^\zeta(\mathcal{C})$ and $\Pi_{\text{rem}}^\zeta(\mathcal{C})$ are functions of the microscopic configurations of $\mathcal{S}$, and depend on the exchange mechanism ζ of the reservoir. Coexistence obtains when the particle current $J_N(\mu^*; \{\tilde{p}_\mathcal{C}\}) = 0$, in which case we have

$$\epsilon e^{\Delta N_\zeta \mu^*} \sum_\mathcal{C} \pi_{\text{ins}}^\zeta(\mathcal{C}) \tilde{p}_\mathcal{C} - \epsilon \sum_\mathcal{C} \pi_{\text{rem}}^\zeta(\mathcal{C}) \tilde{p}_\mathcal{C} = 0, \quad (3.3)$$

where $\pi_{\text{ins}}^\zeta(\mathcal{C}) \equiv \frac{\Pi_{\text{ins}}^\zeta(\mathcal{C})}{\mathcal{N}_\zeta}$, and $\pi_{\text{rem}}^\zeta(\mathcal{C}) \equiv \frac{\Pi_{\text{rem}}^\zeta(\mathcal{C})}{\mathcal{N}_\zeta}$. Therefore,

$$\mu^*(\{\tilde{p}_\mathcal{C}\}) = \frac{1}{\Delta N_\zeta} \ln \frac{\sum_\mathcal{C} \pi_{\text{ins}}^\zeta(\mathcal{C}) \tilde{p}_\mathcal{C}}{\sum_\mathcal{C} \pi_{\text{rem}}^\zeta(\mathcal{C}) \tilde{p}_\mathcal{C}}. \quad (3.4)$$

The coexistence condition relates μ^* to macroscopic stationary means of functions defined on the configuration space of the NNE lattice gas. If $\tilde{p}_\mathcal{C}$ is computed for a fixed particle number, that is, using $\tilde{p}_{\mathcal{C}|N}$, we have

$$\tilde{\pi}_{\text{ins}}^\zeta(N) \equiv \sum_{\mathcal{C} \in \Gamma(L,N)} \pi_{\text{ins}}^\zeta(\mathcal{C}) \tilde{p}_{\mathcal{C}|N} \quad (3.5)$$

and

$$\tilde{\pi}_{\text{rem}}^\zeta(N) \equiv \sum_{\mathcal{C} \in \Gamma(L,N)} \pi_{\text{rem}}^\zeta(\mathcal{C}) \tilde{p}_{\mathcal{C}|N}. \quad (3.6)$$

We can interpret the resulting effective chemical potential as the μ_ζ^* value of the reservoir $\mathcal{R}_\zeta$ that coexists with $\mathcal{S}$. As noted above, this is *virtual* coexistence: No particles are, in fact, exchanged, but one can associate this value of μ^* with the system $\mathcal{S}$, just as in Widom's test-particle insertion method [21].

By contrast, if $\mathcal{S}$ exchanges particles with $\mathcal{R}_\zeta$, N fluctuates, and $\tilde{p}_\mathcal{C}$ corresponds to the fixed-μ^* description, so

$$\langle \pi_{\text{ins}}^\zeta \rangle \equiv \sum_\mathcal{C} \pi_{\text{ins}}^\zeta(\mathcal{C}) \tilde{p}_\mathcal{C}, \quad (3.7)$$

and similarly for $\langle \pi_{\text{rem}}^\zeta \rangle$, in which all configurations $\mathcal{C}$ are included, for all possible values of N. In this case, the value μ^* is imposed upon $\mathcal{S}$ through coexistence with the reservoir, and the stationary means attain values such that Eq. (3.4) holds. In the weak-exchange limit, the fixed-μ^* distribution can be written as $\tilde{p}_\mathcal{C} = \tilde{p}_{\mathcal{C}|N} \tilde{P}_N$, where N is the number of occupied sites in configuration $\mathcal{C}$. Thus,

$$\langle \tilde{\pi}_{\text{ins}}^\zeta \rangle = \sum_N \left[\sum_{\mathcal{C} \in \Gamma(L,N)} \pi_{\text{ins}}^\zeta(\mathcal{C}) \tilde{p}_{\mathcal{C}|N} \right] \tilde{P}_N, \quad (3.8)$$

and similarly for $\langle \pi_{\text{rem}}^{\zeta} \rangle$, where the expression inside the bracket in Eq. (3.8) is exactly the right-hand side of Eq. (3.5), i.e., the stationary mean with fixed particle number.

The foregoing considerations motivate questions (i) and (ii) raised in the Introduction, and that we address in this paper. In this paper, we restrict our attention to two kinds of reservoirs, although many others are possible. The first, $\mathcal{R}_1$, interacts with $\mathcal{S}$ exchanging a single particle per event ($\Delta N_1 = 1$). For $\mathcal{R}_1$, we have $\mathcal{N}_1 = L^2$, $w_{\text{ins}}(\mathcal{R}_1) = \epsilon \exp(\mu^*)$, $w_{\text{rem}}(\mathcal{R}_1) = \epsilon$, $\Pi_{\text{ins}}^1(\mathcal{C}) = N_{\text{op}}(\mathcal{C})$ (number of open sites in $\mathcal{C}$), $\Pi_{\text{rem}}^1(\mathcal{C}) = N$, $\pi_{\text{ins}}^1(\mathcal{C}) = \rho_{\text{op}}(\mathcal{C})$ (open-site density in $\mathcal{C}$) and $\pi_{\text{rem}}^1(\mathcal{C}) = \rho$ (particle density in $\mathcal{C}$). Using these relations in Eq. (3.4), we obtain Eqs. (1.1) and (1.2).

The second kind of reservoir, $\mathcal{R}_2$, interacts with $\mathcal{S}$ inserting two particles at a pair of open second-neighbor sites and removing two particles from a pair of occupied second-neighbor sites ($\Delta N_2 = 2$). In this case, $\mathcal{N}_2 = 2L^2$, $w_{\text{ins}}(\mathcal{R}_2) = \epsilon \exp(2\mu^*)$, $w_{\text{rem}}(\mathcal{R}_2) = \epsilon$, $\Pi_{\text{ins}}^2(\mathcal{C}) = N_{\text{op}}^{(2)}(\mathcal{C})$ (number of open second-neighbor pairs), $\Pi_{\text{rem}}^2(\mathcal{C}) = N^{(2)}(\mathcal{C})$ (number of occupied second-neighbor pairs), $\pi_{\text{ins}}^2(\mathcal{C}) = \rho_{\text{op}}^{(2)}(\mathcal{C})$, and, finally, $\pi_{\text{rem}}^2(\mathcal{C}) = \rho^{(2)}(\mathcal{C})$ (the fraction of second-neighbor pairs in which both sites are occupied).

If reservoir independence holds, as it does in equilibrium, it implies a series of identities between multisite occupation/vacancy probabilities in the TL. For example, equivalence of $\mathcal{R}_1$ and $\mathcal{R}_2$ implies that

$$\frac{\rho}{\tilde{\rho}_{\text{op}}} = \left(\frac{\tilde{\rho}^{(2)}}{\tilde{\rho}_{\text{op}}^{(2)}} \right)^{1/2}. \tag{3.9}$$

More generally, equivalence of reservoirs $\mathcal{R}_{\zeta}$ and $\mathcal{R}_{\xi}$ implies

$$\left(\frac{\tilde{\pi}_{\text{rem}}^{\xi}}{\tilde{\pi}_{\text{ins}}^{\xi}} \right)^{1/\Delta N_{\xi}} = \left(\frac{\tilde{\pi}_{\text{rem}}^{\zeta}}{\tilde{\pi}_{\text{ins}}^{\zeta}} \right)^{1/\Delta N_{\zeta}}. \tag{3.10}$$

Equation (3.10) provides a set of useful identities for lattice gases and other model fluids. In Sec. V. we show that this equivalence does not hold out of equilibrium, even in the infinite-size limit (see Fig. 17).

IV. DESCRIPTION EQUIVALENCE

As discussed in the previous section, when $\mathcal{S}$ is in contact with a particle reservoir $\mathcal{R}_{\zeta}$, the parameters D, V, ζ, μ^*, and ϵ determine the stationary probability distribution on configuration space. This corresponds to the fixed-$(\mu^*, V; D|\zeta, \epsilon)$ description, which, in the WEL, ($\epsilon \to 0$), becomes the fixed-$(\mu^*, V; D|\zeta, \epsilon \to 0)$ description, or simply the *fixed-μ^* description*. The properties of a system $\mathcal{S}$ with no exchange of particles with any other system are given by the fixed-$(N, V; D|\zeta, \epsilon = 0)$ description, or the *fixed-N description*.

A. NESS in the fixed-μ^* description

We consider a particle reservoir $\mathcal{R}$ with dimensionless chemical potential μ^* in contact with a driven NNE lattice gas, denoted by $\mathcal{S}$. At each exchange event between $\mathcal{S}$ and $\mathcal{R}$, a single particle is transferred. The master equation governing

$w(0, +1) \quad w(1, +1) \quad w(2, +1) \quad w(N_{\text{max}} - 1, +1)$

$w(1, -1) \quad w(2, -1) \quad w(3, -1) \quad w(N_{\text{max}}, -1)$
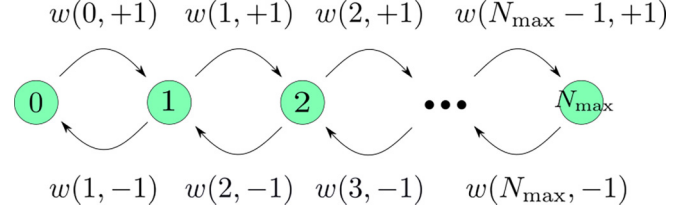
FIG. 3. Stochastic process for the random variable N, the number of particles in $\mathcal{S}$. Each circle represents a state of N. Transition rates are denoted by $w(N, \Delta N)$. The process $N(t)$ is subject to reflecting boundaries at 0 and N_{max}.

P_N, the probability distribution of N is

$$\frac{dP_N(t)}{dt} = \sum_{\Delta N = \pm 1} [w(N', \Delta N)P_{N'}(t) - w(N, \Delta N)P_N(t)], \tag{4.1}$$

where $N' = N - \Delta N$, and $w(N, +1)$ [$w(N, -1)$] denotes the insertion (removal) rate given N. Thus, Eq. (4.1) can be written

$$\frac{dP_N(t)}{dt} = w(N + 1, -1)P_{N+1}(t) + w(N - 1, +1)P_{N-1}(t)$$
$$- [w(N, -1) + w(N, +1)]P_N(t). \tag{4.2}$$

Since $\mathcal{S}$ is in weak contact with $\mathcal{R}$, all exchanges occur when $\mathcal{S}$ is in the NESS with N particles. Therefore, the macroscopic insertion and removal rates are given by

$$w(N, +1) = \sum_{\mathcal{C} \in \Gamma(L, N)} w_{\text{ins}}(\mathcal{R}) \tilde{p}_{\mathcal{C}|N} = \epsilon z \tilde{\rho}_{\text{op}}(N) \tag{4.3}$$

and

$$w(N, -1) = \sum_{\mathcal{C} \in \Gamma(L, N)} w_{\text{rem}}(\mathcal{R}) \tilde{p}_{\mathcal{C}|N} = \epsilon \rho, \tag{4.4}$$

where $z \equiv e^{\mu^*}$.

Given the reflecting barriers at $N = 0$ and $N = N_{\text{max}}$, as illustrated in Fig. 3, in the stationary state *of the exchange process* (not to be confused with the NESS of $\mathcal{S}$), the probability current between two successive values of N must vanish. Thus, the exchange process satisfies a macroscopic detailed balance relation. Denoting the stationary probability distribution of N by $\tilde{P}_N$, we have

$$\tilde{P}_{N-1} w(N - 1, 1) = \tilde{P}_N w(N, -1). \tag{4.5}$$

We write $\tilde{P}_N$ as

$$\tilde{P}_N = \frac{W_N}{\Xi(z)}, \tag{4.6}$$

where W_N is a weight associated with state N and $\Xi(z) = \sum_{N=0}^{N_{\text{max}}} W_N$. From Eq. (4.5),

$$W_N = z \frac{\tilde{N}_{\text{op}}(N - 1)}{N} W_{N-1}, \tag{4.7}$$

and setting $W_0 = 1$, we have

$$W_N = z^N \frac{\Psi(N, D)}{N!}, \tag{4.8}$$

where $\Psi(N, D) \equiv \prod_{i=0}^{N-1} \tilde{N}_{\text{op}}(i)$.

This implies the equilibriumlike relations

$$\frac{\partial \ln \Xi}{\partial \mu^*} = \langle N \rangle \tag{4.9}$$

and

$$\frac{\partial \langle N \rangle}{\partial \mu^*} = \langle N^2 \rangle - \langle N \rangle^2, \tag{4.10}$$

which reflect the fact that the exchange rates between $\mathcal{S}$ and $\mathcal{R}$ satisfy detailed balance. It is nevertheless important to note that $\Psi(N, D)$ depends on D, as does $\Xi = \Xi(z, D)$.

B. Macrostate, thermodynamic, and measure equivalence

There are three levels of description equivalence [13]: macrostate, thermodynamic, and measure equivalence. Macrostate equivalence means that averages of physical quantities taken in the two ensembles are equal in the TL. Thermodynamic equivalence means that the thermodynamic quantities (i.e., free energy, intensive parameters) used to describe system properties lead to the same physical predictions. Since the model used has only one relevant parameter, the dimensionless chemical potential, macrostate equivalence implies thermodynamic equivalence. Finally, measure equivalence means that the probability distributions that describe each of the statistical ensembles are equivalent. That is, although each ensemble is defined on a distinct configuration space, a subspace of possible configurations is selected by the shape of the probability distribution $\tilde{P}_N$.

Recall that in the weak-exchange limit, all exchanges between $\mathcal{S}$ and $\mathcal{R}$ occur with $\mathcal{S}$ in its N-particle steady-state. This implies that the fixed-N and fixed-μ^* distributions are related via

$$\tilde{p}_{\mu^*}(\mathcal{C}) = \tilde{p}_{\mathcal{C}|N} \tilde{P}_N. \tag{4.11}$$

In what follows it will be convenient write the stationary probability $\tilde{P}_N$ as a function of particle density, i.e., $\tilde{P}(\rho)$, where $\rho = N/L^2$. In the TL, ρ is a continuous variable with probability density $\tilde{\mathcal{P}}(\rho)$. If $\tilde{\mathcal{P}}(\rho) \to \delta(\rho - \langle \rho \rangle)$ in the TL and macrostate equivalence holds, then measure equivalence also holds. Moreover, $\tilde{\mathcal{P}}(\rho)$ can then be described by a large-deviation function $I(\rho)$, such that in the TL, $\tilde{\mathcal{P}}(\rho) \asymp \exp(-L^2 I(\rho))$, where the symbol $\asymp$ is used to emphasize that when $L \to \infty$, the decaying exponential dominates the behavior of $\tilde{\mathcal{P}}(\rho)$ [22].

In equilibrium, description equivalence is well established for the NNE model since the interactions are short-ranged [13,23]. In the following, we compare how description equivalence emerges as we increase the system size, in equilibrium and under a drive.

C. $\Xi(z, D)$ and the conditions for description equivalence

The function $\Xi(z, D)$ can be written as

$$\Xi(z, D) = \sum_{N=0}^{N_{\max}} W_N(z, D) = \sum_{N=0}^{N_{\max}} z^N \Lambda(N, D), \tag{4.12}$$

where $\Lambda(N, D) \equiv \Psi(N, D)/N!$. In the TL, $L \to \infty$, let $N = L^d \rho$ and $\tilde{N}_{\mathrm{op}}(N) = \tilde{\rho}_{\mathrm{op}}(\rho) L^d$. Then,

$$\Xi(z, D) = L^d \int d\rho \, \exp\{L^d[\mu^* \rho + \lambda(\rho, D)]\}, \tag{4.13}$$

where we have defined

$$\lambda(\rho, D) \equiv \frac{1}{L^d} \ln \Lambda(L^d \rho, D). \tag{4.14}$$

For description equivalence to hold, $W_N(z, D)$ must have a unique maximum in the TL. Using Stirling's approximation, $\ln N! \approx N \ln N - N$, we obtain

$$\ln W_N(z, D) \cong L^d \left\{ \rho \ln z - \rho \ln \rho + \rho + \int_0^\rho \ln \tilde{\rho}_{\mathrm{op}}(\rho') d\rho' \right\}. \tag{4.15}$$

Maximizing $\ln W_N(z)$ with respect to ρ yields the familiar relation $\mu^* = \ln[\rho/\tilde{\rho}_{\mathrm{op}}(\rho)]$, while maximizing the integrand of Eq. (4.13) yields

$$\frac{\partial \lambda(\rho)}{\partial \rho} = -\mu^*. \tag{4.16}$$

The condition that (4.16) has a unique solution is that $\lambda(\rho)$ be concave, i.e., $\partial^2 \lambda(\rho)/\partial \rho^2 \leqslant 0$. Noting that

$$\frac{\partial^2 \lambda(\rho)}{\partial \rho^2} = -\frac{\partial \mu^*}{\partial \rho} = -\frac{1}{\rho} + \frac{1}{\tilde{\rho}_{\mathrm{op}}(\rho)} \frac{\partial \tilde{\rho}_{\mathrm{op}}(\rho)}{\partial \rho}, \tag{4.17}$$

we see that a sufficient condition for the concavity of λ is that

$$\frac{\partial \tilde{\rho}_{\mathrm{op}}(\rho)}{\partial \rho} \leqslant 0, \tag{4.18}$$

that is, that the mean density of open sites be a nonincreasing function of particle density, a relation that seems intuitively obvious even if we lack a formal proof. Below we provide numerical evidence for the concavity of $\lambda(\rho)$.

D. Results

1. Macrostate equivalence

To test macrostate equivalence, we calculate μ^* in the fixed-N description for diverse values of ρ and D using Eq. (1.1). Then, we compute $\tilde{P}_N$ for these μ^* values using Eqs. (4.6) and (4.8), and finally determine the stationary macroscopic means in the fixed-μ^* description. Thus, we ask whether the relations

$$\rho = \langle \rho \rangle, \tag{4.19}$$

$$\tilde{\rho}_{\mathrm{op}}(\rho) = \langle \tilde{\rho}_{\mathrm{op}}(\rho) \rangle, \tag{4.20}$$

$$\tilde{\rho}^{(2)}(\rho) = \langle \tilde{\rho}^{(2)}(\rho) \rangle, \tag{4.21}$$

$$\tilde{\rho}_{\mathrm{op}}^{(2)}(\rho) = \langle \tilde{\rho}_{\mathrm{op}}^{(2)}(\rho) \rangle, \tag{4.22}$$

hold to within numerical uncertainty.

Figure 4 shows the differences between stationary macroscopic quantities in equilibrium ($D=0$) for lattice sizes $L = 10, 20, 28, 56, 64, 96, 128, 160$. In equilibrium, as expected, the difference between corresponding quantities in the two descriptions decreases as L grows. Figure 5, for
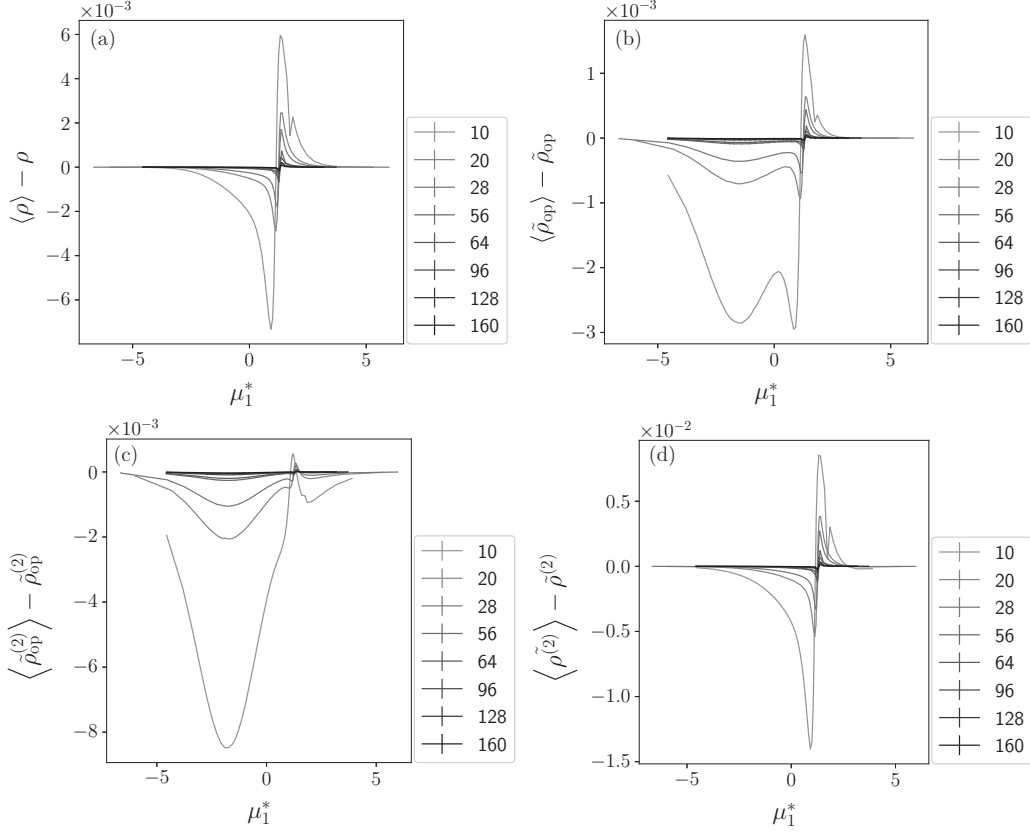
FIG. 4. NNE model in equilibrium. Differences between macroscopic means computed in the fixed-N and fixed-μ^* ensembles as a function of μ^* for system sizes as indicated. (a) differences in density, (b) open-site density, (c) density of second-neighbors pairs, (d) density of occupied pairs of second neighbors. Error bars are smaller than 10^{-4}.

$D = 1$, shows similar behavior in the maximum-drive case. In both figures, the error bars are smaller than 10^{-4}, and can barely be seen. Figure 6 shows the global deviation $\Delta\rho \equiv \max(\langle\rho\rangle - \tilde\rho) - \min(\langle\rho\rangle - \tilde\rho)$ (top left), as well as $\Delta\rho_{\mathrm{op}}$ (top right), $\Delta\rho_{\mathrm{op}}^{(2)}$ (bottom left), $\Delta\rho^{(2)}$ (bottom right), defined analogously, as functions of $1/L$. The blue circles correspond to $D = 0$ (equilibrium), green stars to maximum drive, $D = 1$. The tendency to decay as L increases is clear for all four quantities studied, in or out of equilibrium. These results are evidence that in the TL, macrostates are identical in the two descriptions.

2. Concavity of $\lambda(\rho, D)$

Using simulation data, we compute $\lambda(\rho, D)$ [Eq. (4.14)]. Figure 7 (left panel) compares $\lambda(\rho, D)$ in equilibrium (solid line) and for $D = 1$ (broken line), for $L = 160$. Both curves are clearly concave. The right panel of this figure shows $\lambda(\rho, D = 1)$ for diverse lattice sizes, suggesting convergence to a limiting function as $L \to \infty$.

Figure 8 shows $\partial\tilde\rho_{\mathrm{op}}/\partial\rho$ estimated via finite differences for $L = 160$, for $D = 0$ (blue curve) and $D = 1$ (broken orange curve); the maximum value of the derivative does not change significantly with lattice size. These results are numerical evidence of the concavity of $\lambda(\rho, D)$, and hence, description equivalence, for nonequilibrium steady states states as well as in equilibrium.

3. Probability density

We turn our attention to the probability density $\tilde{\mathcal{P}}(\rho)$, which is approximated from the discrete probability distribution $\tilde{P}(\rho)$ as follows. Since, for a square lattice of linear size L, the maximum number of particles is $N_{\max} = L^2/2$ (for even L), and the number of possible density values is $N_{\max} + 1$, we define $\delta\rho$ as

$$\delta\rho \equiv \frac{\rho_{\max} - \rho_{\min}}{N_{\max} + 1} = \frac{0.5}{N_{\max} + 1}, \qquad (4.23)$$

and then write $\tilde{\mathcal{P}}(\rho)$ as

$$\tilde{\mathcal{P}}(\rho) = \frac{\tilde{P}(\rho)}{\delta\rho}. \qquad (4.24)$$

Figure 9 (left panel) shows $\tilde{\mathcal{P}}(\rho)$ for $D = 1$ and $\mu^* = 1.15$ and various system sizes. As L increases, the probability density accumulates around the mean. The maximum value increases with L, suggesting a tendency toward a δ distribution. Defining $\hat\rho \equiv L(\rho - \rho^*)$, where ρ^* is the value of ρ that maximizes $\tilde{\mathcal{P}}(\rho)$, and $\hat{Q} \equiv L^{-1}\tilde{\mathcal{P}}(\rho)$, we verify the tendency to a δ function in Fig. 10, which shows that the maximum of $\hat{Q}$ tends to a constant when $L \to \infty$, both in equilibrium and under maximum drive. All curves are centered at zero, confirming that $\langle\rho\rangle = \rho^*$.

Finally, we consider a numerical approximation for the large-deviation function $I(\rho) = -\ln\tilde{\mathcal{P}}(\rho)/L^2$. Figure 9 (cen-
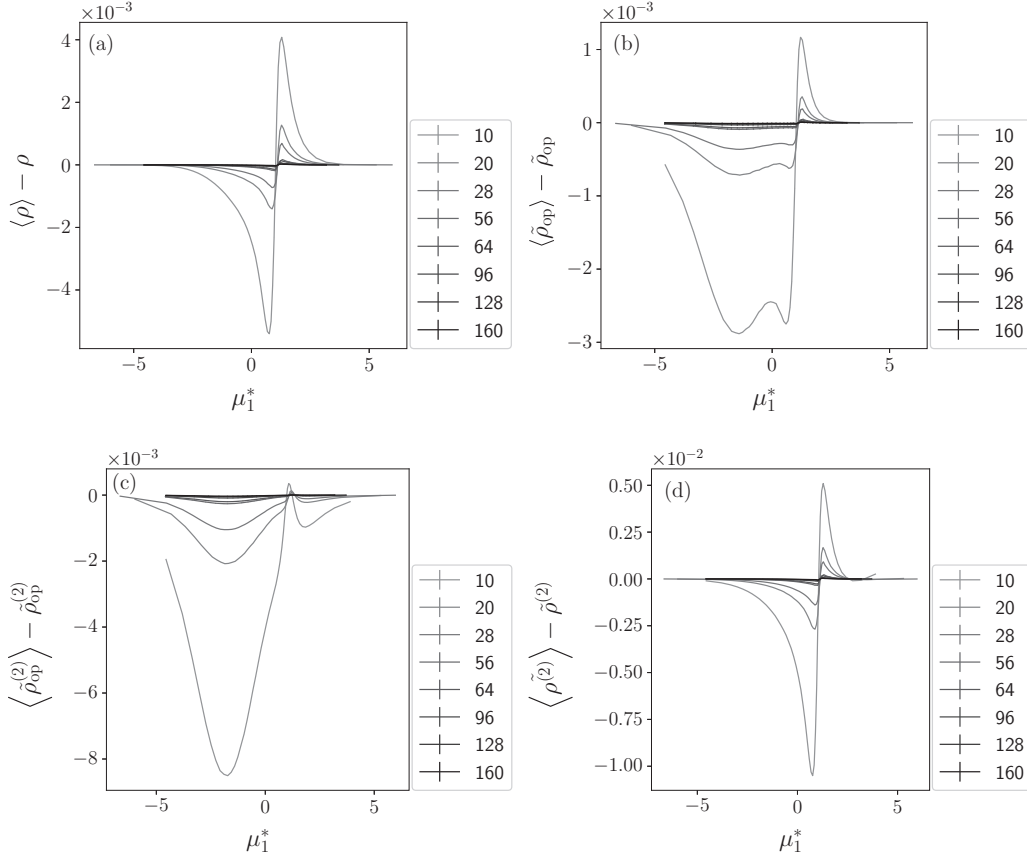
FIG. 5. NNE model under maximum drive. Differences between macroscopic means computed in the fixed-N and fixed-μ^* descriptions as a function of μ^* for system sizes as indicated. (a) Differences in density, (b) open-site density, (c) density of second-neighbors pairs, (d) density of occupied pairs of second neighbors. Error bars are smaller than 10^{-4}.

tral panel) shows $I(\rho)$ for diverse values of L. One expects $I(\rho)$ to be nonnegative, with a root at ρ^*. Indeed, this property is asymptotically approached as L increases. Figure 9 (right panel) shows that $I_{\min}$ approaches zero as L increases. We find similar results for μ^* in $[-4, 4]$, and D in $[0,1]$.

E. Discussion

The above results lead us to conclude that description equivalence holds in the NNE model under a drive, as well as in equilibrium. Previously, the effective chemical potential determined in the fixed-N case (1.1) was shown to have predictive power for systems exchanging particles [3], thereby suggesting equivalence. The present results sustain this conclusion and justify the use of (1.1) to measure the chemical potential of NESS in isolation. Our results for the NNE model are in accord with Ref. [15] in which the grand canonical ensemble is derived using the assumption that the systems of interest can be described by a large-deviation principle in the TL. The authors of Ref. [15] found that similar results hold in general: (a) a probability distribution for N with the same structure as the equilibrium one; (b) given that this probability distribution is described by a large deviation function (for them, an assumption, for us, a result) one has macroscopic equivalence; (c) the chemical potential obtained from minimizing the rate function, $I(\rho)$, is equal to the one we obtain using the zero-current condition.

V. RESERVOIR INDEPENDENCE

A. Two-reservoir scheme

Consider a NNE lattice gas $\mathcal{S}$ in a steady state, in contact via weak global exchange with two reservoirs, $\mathcal{R}_1$ and $\mathcal{R}_2$, with chemical potentials μ_1^* and μ_2^*, respectively. The former exchanges single particles with $\mathcal{S}$, while the latter inserts a pair of particles at pairs of open second-neighbor sites and removes a pair of particles from occupied second-neighbor sites. The insertion and removal rates for each reservoir satisfy detailed balance, as discussed in Sec. III. $w_{\mathrm{ins}}(\mathcal{R}_1)$ and $w_{\mathrm{rem}}(\mathcal{R}_1)$ carry a factor ε_1 representing the overall exchange rate with $\mathcal{R}_1$; similarly, $w_{\mathrm{ins}}(\mathcal{R}_2)$; $w_{\mathrm{rem}}(\mathcal{R}_2)$ carry a factor ε_2. In the weak-exchange limit, both ε_1 and ε_2 tend to zero, with $\varepsilon_1/\varepsilon_2 \equiv \epsilon$. Figure 11 illustrates $\mathcal{S}$ in contact with $\mathcal{R}_1$ and $\mathcal{R}_2$.

The macroscopic master equation describing the two-reservoir scheme is

$$\frac{dP_N(t)}{dt} = \sum_{\Delta N = \pm 1, \pm 2} [w(N', \Delta N)P_{N'}(t) - w(N, \Delta N)P_N(t)]. \tag{5.1}$$

As before, $N' = N - \Delta N$. The macroscopic rates for exchange with $\mathcal{R}_2$ are

$$w(N, +2) = \sum_{\mathcal{C} \in \Gamma(L,N)} w_{\mathrm{ins}}(\mathcal{R}_2) \, \tilde{p}_{\mathcal{C}|N} = \varepsilon_2 z_2^2 \, \tilde{\rho}_{\mathrm{op}}^{(2)}(N) \tag{5.2}$$
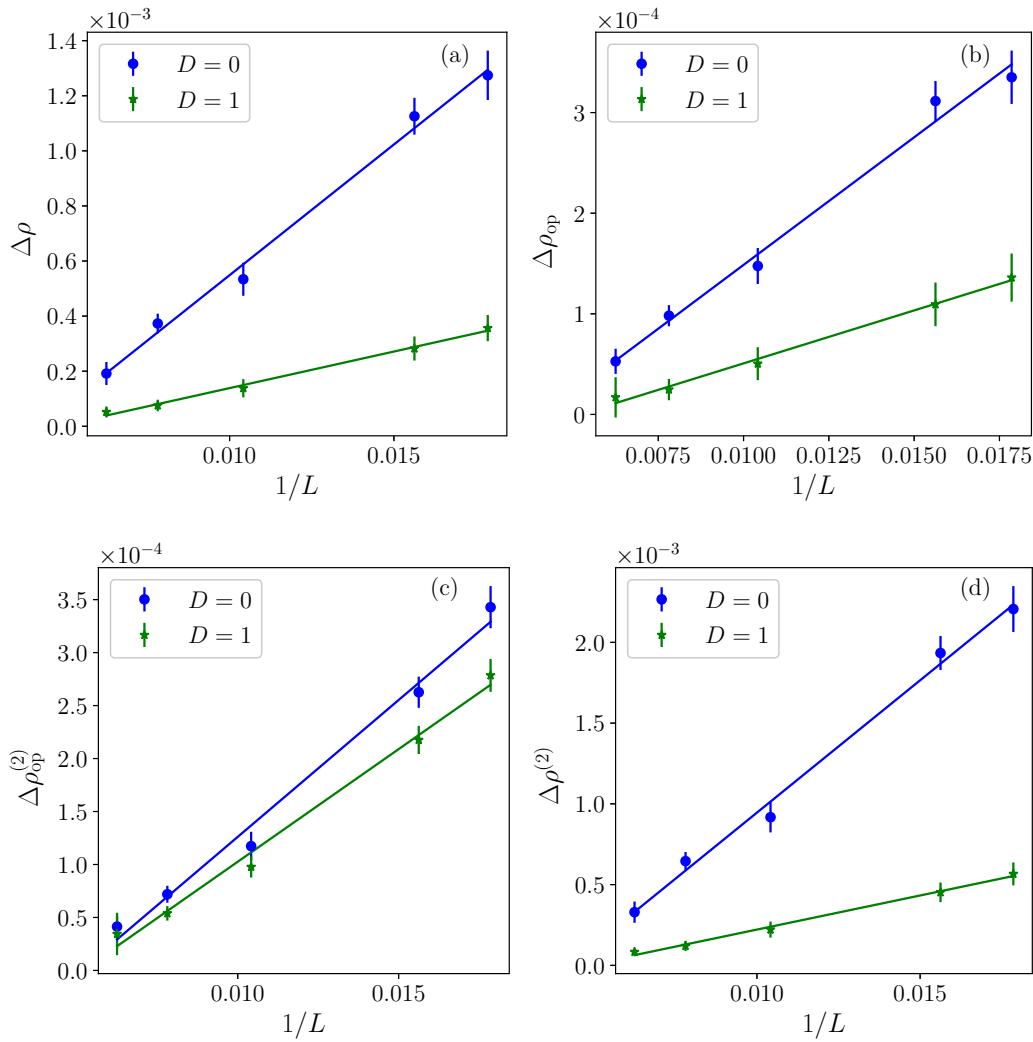
FIG. 6. (a) $\Delta\rho$, (b) $\Delta\rho_{\mathrm{op}}$, (c) $\Delta\rho_{\mathrm{op}}^{(2)}$, (d) $\Delta\rho^{(2)}$ versus $1/L$, for $L = 56, 64, 96, 128, 160$. Here, $\Delta\rho \equiv \max\{\langle\rho\rangle - \rho\} - \min\{\langle\rho\rangle - \rho\}$, and analogously for the others quantities. Blue circles: $D = 0$; green stars: $D = 1$. The lines are linear fits to the data.
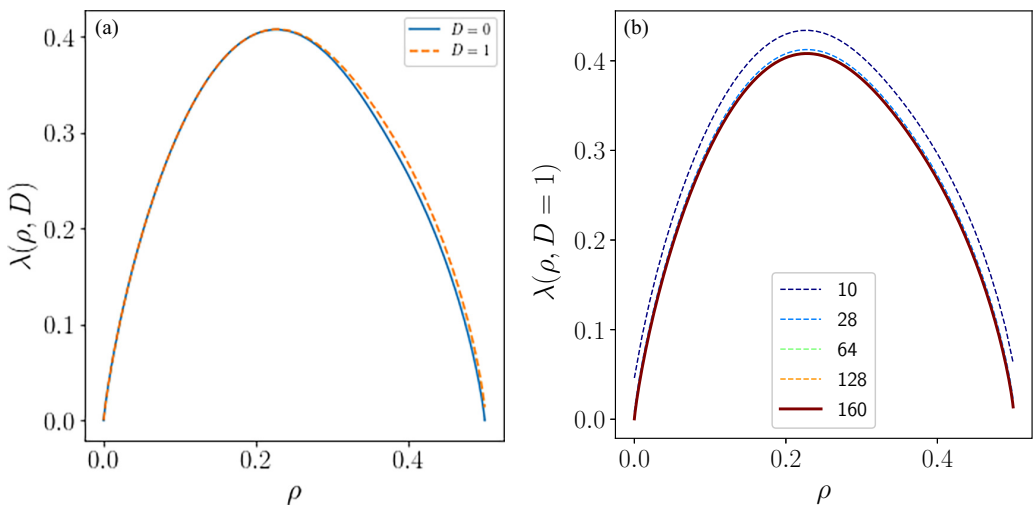

FIG. 7. (a) $\lambda(\rho, D)$ versus ρ in equilibrium (continuous blue curve) and for $D = 1$ (dashed orange curve), $L = 160$. (b) Convergence of $\lambda(\rho)$ with increasing system size. The dashed curves are for $L = 10, 28, 64,$ and 128. These curves accumulate near the thicker continuous curve ($L = 160$).
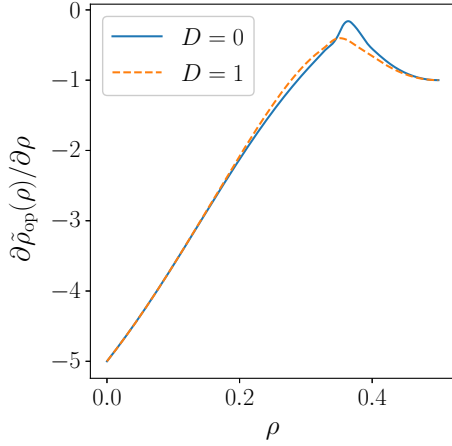
FIG. 8. Derivative of open-site density $\tilde{\rho}_{op}(\rho)$ as function of density ρ for lattice size $L = 160$. The maximum value, in equilibrium (continuous blue curve) and away from equilibrium (dashed orange curve) is never greater than zero, so the inequality (4.18) always holds.

and

$$w(N, -2) = \sum_{\mathcal{C} \in \Gamma(L,N)} w_{rem}(\mathcal{R}_2)\, \tilde{p}_{\mathcal{C}|N} = \varepsilon_2\, \tilde{\rho}^{(2)}(N). \quad (5.3)$$

We choose the time unit such that $\varepsilon_2 = 1$, and therefore, $\varepsilon_1 = \epsilon$. Thus $\epsilon = 0$ corresponds to $\mathcal{S}$ in contact with $\mathcal{R}_2$ only, and $\epsilon \to \infty$ to contact with $\mathcal{R}_1$ only. Note that for $\epsilon = 0$, configuration space is divided into two mutually inaccessible regions, one with N even, the other with N odd. Therefore, to probe the small-ϵ regime, it is more convenient to study the *limit* $\epsilon \to 0$, rather than setting ϵ to zero.

Let J_{N_1} and J_{N_2} denote the particle currents between $\mathcal{S}$ and $\mathcal{R}_1$ and $\mathcal{R}_2$, respectively. The currents, taken as positive when the net flux is *into* $\mathcal{S}$, are

$$J_{N_1} = \epsilon[z_1\langle\tilde{\rho}_{op}\rangle - \langle\rho\rangle] \quad (5.4)$$

and

$$J_{N_2} = \left[z_2^2\langle\tilde{\rho}_{op}^{(2)}\rangle - \langle\tilde{\rho}^{(2)}\rangle\right]. \quad (5.5)$$

The total particle current $J_N = J_{N_1} + J_{N_2}$ must vanish in the stationary state. Reservoir independence holds if $\mu_1^* = \mu_2^* = \mu^*$ implies $J_{N_1} = J_{N_2} = 0$ for all values of μ^*.

B. Results

In this subsection, we report results based on the stationary solution of the master equation, (V.1). This is achieved in two steps: First, we obtain precise estimates of the transition rates, $w(N, \Delta N)$ via Monte Carlo simulation (see the last two paragraphs of Sec. II). Then we solve the master equation using the iterative method introduced in Ref. [24].

1. $\mu_1^* = \mu_2^*$

We study the case of equal chemical potentials, $\mu_1^* = \mu_2^* = \mu^*$, for $\epsilon = 0.01, 0.1, 0.5, 1$, and $\mu^* \in [-4, 2]$. Remarkably, we find that when $\mathcal{S}$ is out of equilibrium ($D > 0$), *there is a nonzero particle current from one reservoir to the other*. Particles are transferred from $\mathcal{R}_2$ to $\mathcal{R}_1$ for small μ^*, and in the opposite sense for larger values. Figure 12 shows J_{N_1} as a function of μ^* and D, for $\epsilon = 1$. (The upper panel is for $L = 28$, the bottom for $L = 160$.) The current increases with D, exhibiting a maximum for $\mu^* \approx 0.9$. Although the numerical values for the two sizes are different, they have the same order of magnitude and very similar behaviors. Varying ϵ, the intensity of the current varies, but its qualitative behavior remains the same.

Figure 13 shows the currents J_{N_1} (blue line), J_{N_2} (orange line), and $J_N = J_{N_1} + J_{N_2}$ (green line) as a function of D for $\mu^* = 0.9$. $|J_{N_1}| \propto D^2$ near $D = 0$, as required by symmetry, and approaches a linear dependence for larger drives. The particle current between reservoirs is nonzero except for very specific combinations of μ^*, D, and ϵ. These results demonstrate that, out of equilibrium, reservoir independence no longer holds!
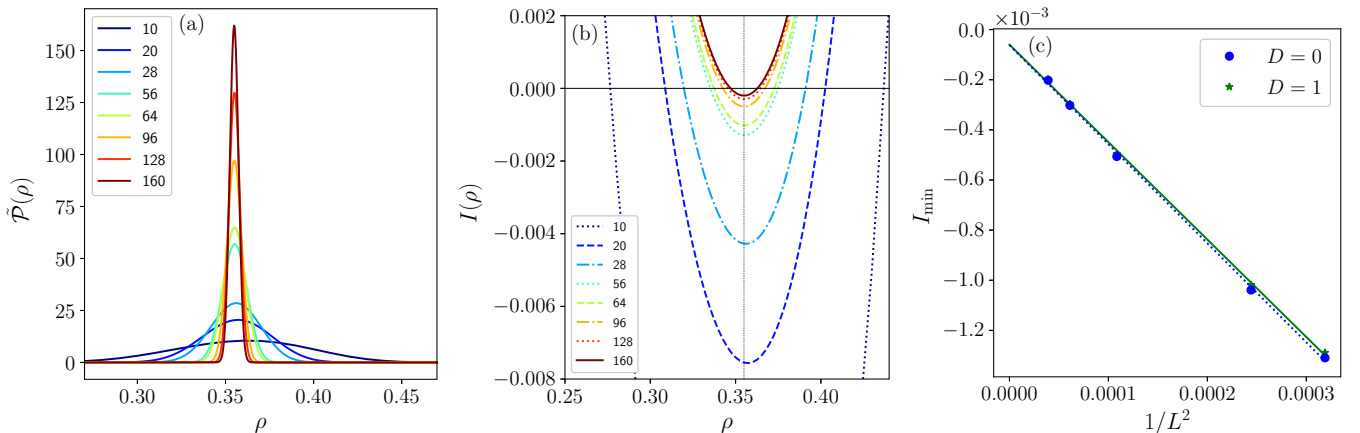

FIG. 9. (a) Probability density $\tilde{\mathcal{P}}(\rho)$ [Eq. (4.24)] for lattice sizes as indicated. The maximum value of $\tilde{\mathcal{P}}(\rho)$ increases monotonically with L. (b) Large-deviation function $I(\rho)$ near its minimum. $I(\rho)$ is expected to have a single root exactly at ρ^*, the value of ρ that maximizes $\tilde{\mathcal{P}}(\rho)$. (c) I_{min} versus $1/L^2$ for $L = 64, 96, 128, 160$. Symbols are data and lines linear fits. Blue circles and broken line: $D = 0$; green stars and continuous line: $D = 1$.
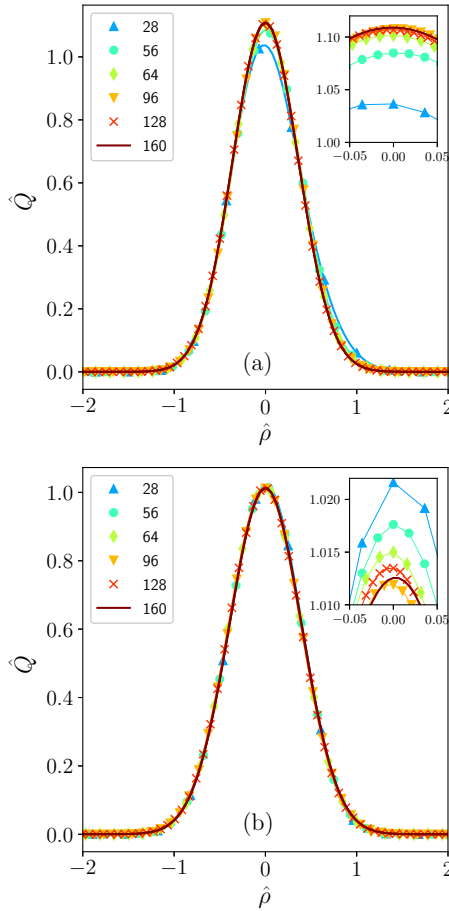
FIG. 10. Scaling functions, $\hat{Q} \equiv L^{-1}\tilde{\mathcal{P}}(\rho)$, versus scaled density $\hat{\rho} \equiv L(\rho - \rho^*)$ for $\mu^* = 1.15$; the collapse of the curves is almost perfect. The insets show details near the maximum. (a) Equilibrium. (b) Maximum drive.

2. $\mu_1^* \neq \mu_2^*$

Given that, under a nonzero drive, there is a particle current from one reservoir to the other for $\mu_1^* = \mu_2^*$, we ask if it is possible, given μ_1^* and D, to adjust μ_2^* such that the particle current between reservoirs vanishes. For example, when $\mu_1^* = \mu_2^* = 0.9$, particles flow from $\mathcal{R}_1$ to $\mathcal{R}_2$. One naturally expects this flux to decrease as one increases μ_2^* and to vanish
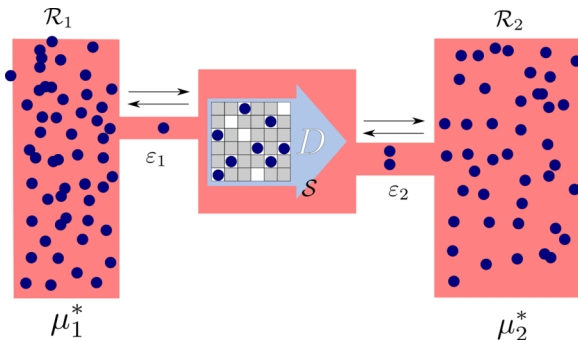

FIG. 11. Two-reservoir scheme. Reservoir $\mathcal{R}_i$ with dimensionless chemical potential μ_i^* exchanges particles with $\mathcal{S}$ at rate ε_i ($i = 1, 2$).
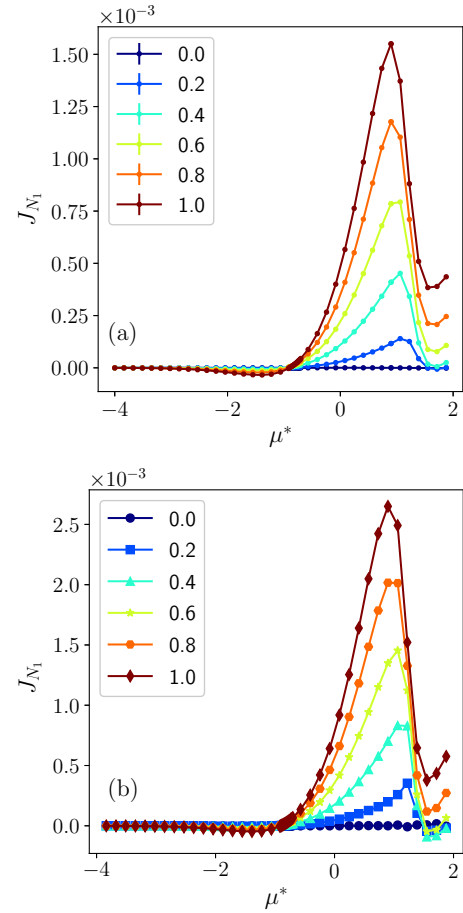

FIG. 12. Stationary particle current from $\mathcal{R}_1$ to $\mathcal{S}$ versus dimensionless chemical potential μ^* for $\epsilon = 1$, and $L = 28$ (a) and $L = 160$ (b) for drives D indicated in the key. (Note that this is the same current delivered to $\mathcal{R}_2$.) In general, there is a particle current from one reservoir to the other, unless $D = 0$ (equilibrium).

for some $\mu_2^* = \overline{\mu_2^*}$, at which point $J_{N_1} = J_{N_2} = 0$ and the two reservoirs coexist simultaneously with $\mathcal{S}$.
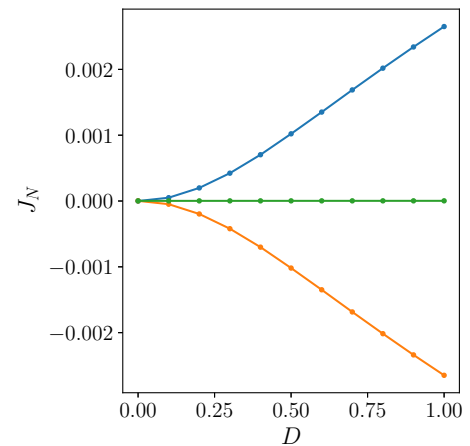

FIG. 13. Particle currents to $\mathcal{S}$, J_{N_1} from $\mathcal{R}_1$ (upper) to $\mathcal{S}$, and J_{N_2} from $\mathcal{R}_2$ to $\mathcal{S}$ (lower) versus drive D for $\mu^* = 0.9$, $\epsilon = 1$ and $L = 160$. The green horizontal curve denotes $J_{N_1} + J_{N_2}$, which is always zero in the stationary state.
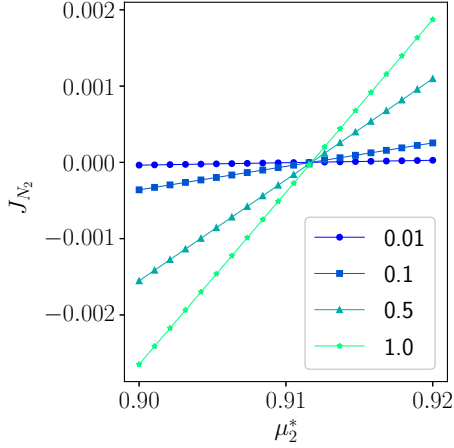
FIG. 14. Current J_{N_2} from $\mathcal{R}_2$ to $\mathcal{S}$ versus μ_2^*, for $\mathcal{R}_1$ at fixed chemical potential $\mu_1^* = 0.9$. Each line is for a distinct value of ϵ as indicated. Negative values of J_{N_2} mean that $\mathcal{R}_2$ receives particles, and vice versa. The value of μ_2^* such that $J_{N_2} = 0$ is independent of ϵ.

We study the particle flux between reservoirs for $\mu_1^* = 0.7$, 0.8, 0.9, and 1.0, (i.e., values exhibiting relatively strong violations of reservoir equivalence) and diverse values of ϵ. We use J_{N_2} to measure of flux between $\mathcal{R}_1$ and $\mathcal{R}_2$: If $J_{N_2} < 0$, $\mathcal{R}_2$ receives particles from $\mathcal{R}_1$, and vice versa. For each μ_1^*, we evaluate the current J_{N_2} for $\mu_2^* = \mu_1^* + \Delta\mu^*$, for a series of positive $\Delta\mu^*$ values. Figure 14 shows J_{N_2} versus μ_2^* for $L = 160$ and $\mu_1^* = 0.9$; J_{N_2} increases linearly with $\Delta\mu^*$. Using linear interpolation, we estimate $\overline{\mu_2^*} \approx 0.9117$. A remarkable fact is $\overline{\mu_2^*}$ has nearly the same value, independent of ϵ: All curves appear to cross zero at the same point. Finally, $\overline{\mu_2^*}$ depends on L in a manner suggesting convergence as L increases, as expected since the stationary means depend weakly on L.

If $\mathcal{S}$ is in equilibrium ($D = 0$), it coexists simultaneously with $\mathcal{R}_1$ and $\mathcal{R}_2$ when they share the same value of μ^*. In this case, the stationary probability distribution $\tilde{P}_N$ is the same, whether $\mathcal{S}$ is in contact with both reservoirs, or only with $\mathcal{R}_1$.

FIG. 16. Relative entropy versus dimensionless chemical potential μ_2^*, between P_N^1, the probability distribution when only $\mathcal{R}_1$ is connected to $\mathcal{S}$, and P_N^2, the distribution when both reservoirs are connected, for $\mu_1^* = 0.9$. Each line corresponds to a rate ϵ (from darkest to lightest, $\epsilon = 0.01, 0.1, 0.5, 1.0$). (a) equilibrium ($D = 0$); (b) nonequilibrium ($D = 1$). In both cases, the minimum in relative entropy is independent of ϵ.

For $D > 0$, this is no longer the case. Figure 15 compares, for $D = 1$, the probability distribution P_N^1 when $\mathcal{S}$ is only in contact with $\mathcal{R}_1$, with P_N^2, the probability distribution when $\mathcal{S}$ is in contact with both reservoirs. The left panel shows P_N^1 and P_N^2 for $\mu_1^* = \mu_2^* = 0.9$, the center panel for $\mu_1^* = 0.9$ and $\mu_2^* = 0.9117$, all with $\epsilon = 1$. The right panel shows the difference $P_N^2 - P_N^1$ for the two situations, showing that for $\mu_2^* = \overline{\mu_2^*}$, $P_N^2 = P_N^1$. Thus, to obtain equal distributions under a drive, the chemical potentials must differ by $\Delta\mu^*$, whose value depends on D, μ_1^*, and L. (Since the two reservoirs now coexist with $\mathcal{S}$, it is not surprising that the value of $\overline{\mu_2^*}$ is independent of the relative coupling strength ϵ).

For a quantitative comparison between P_N^1 and P_N^2, we analyze the Kullback-Leibler divergence or relative entropy,

$$H_{\text{rel}}\left(P_N^1 \middle| P_N^2\right) = \sum_{N=0}^{N_{\max}} P_N^1 \ln \frac{P_N^1}{P_N^2}, \qquad (5.6)$$
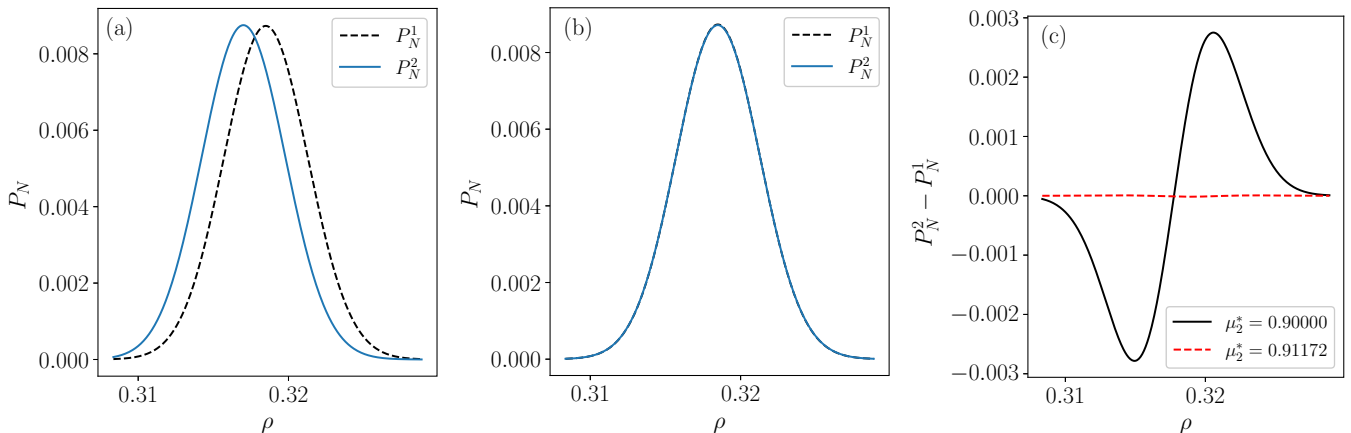

FIG. 15. Panels (a) and (b) show the probability distribution P_N for $\mu_1^* = 0.9$, $D = 1$ and $\epsilon = 1$. The broken black line is P_N^1, the probability distribution when only $\mathcal{R}_1$ is connected to $\mathcal{S}$. The continuous blue line is P_N^2, the probability distribution when both $\mathcal{R}_1$ and $\mathcal{R}_2$ are connected to $\mathcal{S}$. (a) $\mu_2^* = 0.9$, (b) $\mu_2^* = 0.91172$. Panel (c) shows the difference $P_N^2 - P_N^1$ in the two situations. The continuous black line is for $\mu_2^* = 0.9$, the broken red line is for $\mu_2^* = 0.91172$.
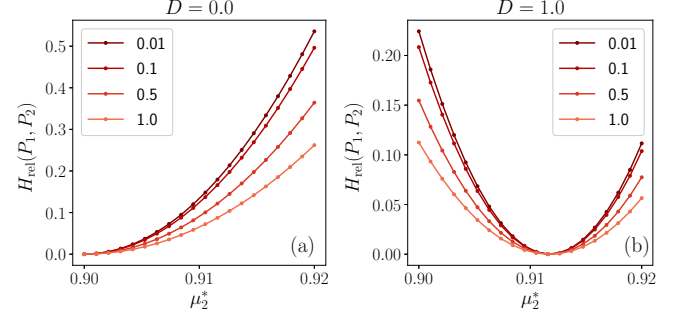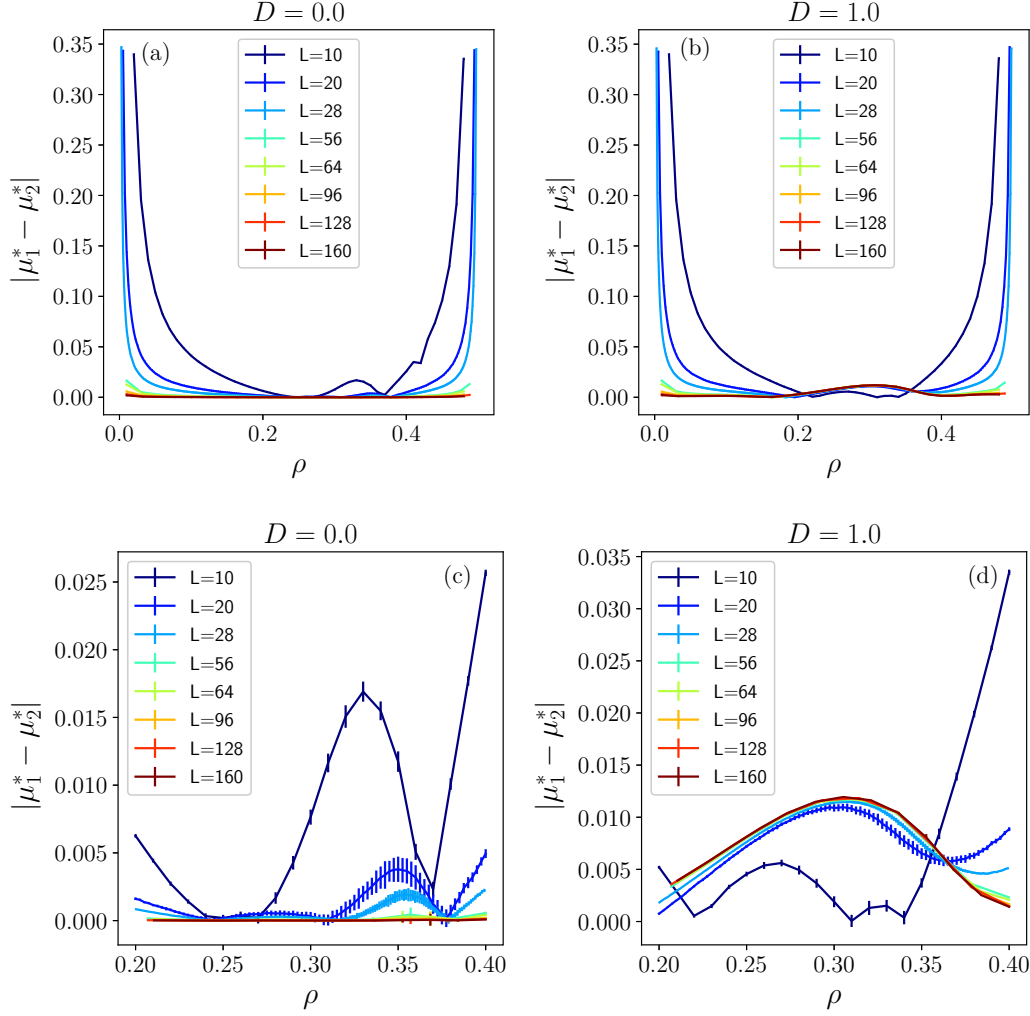
FIG. 17. Dimensionless effective chemical potentials, μ_1^* and μ_2^* computed by virtual coexistence as functions of density, respectively for $\mathcal{R}_1$ and $\mathcal{R}_2$. Panels (a) and (c) are for equilibrium ($D = 0$), with the lower panel highlighting the region of greatest difference; (b) and (d) are for maximum drive ($D = 1$). Out of equilibrium the virtual coexistence method yields $|\mu_1^* - \mu_2^*|$ converging to a nonzero limit as L increases.

as a function of μ_2^*. The left panel in Fig. 16 shows that for $D = 0$ (equilibrium), $P_N^1 = P_N^2$ when $\mu_1^* = \mu_2^* = 0.9$. Any deviation of μ_2^* from μ_1^* leads to $H_{\text{rel}}(P_N^1 | P_N^2) > 0$. Moreover, H_{rel} has a clear dependence on ϵ. The right panel, for $D = 1$ and $\mu_1^* = 0.9$, demonstrates that independence of ϵ and $H_{\text{rel}} \simeq 0$ are observed for $\mu_2^* \approx 0.9117$. Similar behaviors are found for other values of μ_1^*. Inspection of Eqs. (5.4) and (5.5), shows that one can determine $\overline{\mu_2^*}$ directly from stationary means computed using P_N^1. The condition $J_{N_2} = 0$ implies

$$\overline{\mu_2^*} = \frac{1}{2} \ln \frac{\langle \tilde{\rho}^{(2)} \rangle}{\langle \tilde{\rho}_{\text{op}}^{(2)} \rangle}, \tag{5.7}$$

where $\langle \tilde{\rho}^{(2)} \rangle$ and $\langle \tilde{\rho}_{\text{op}}^{(2)} \rangle$ are computed using P_N^1. Thus, for $L = 160$, $\mu_1^* = 0.9$ and $D = 1$, we find $\overline{\mu_2^*} = 0.911718$.

We can use description equivalence and the expressions obtained using virtual exchange to understand these results in the TL. Applying Eq. (3.2) to the two-reservoir setup and the

fixed-N probability distribution, and isolating μ_2^* we find

$$\mu_2^* = \frac{1}{2} \ln \frac{\epsilon(\rho - \tilde{\rho}_{\text{op}} z_1) + \tilde{\rho}^{(2)}}{\tilde{\rho}_{\text{op}}^{(2)}}. \tag{5.8}$$

For μ_2^* to be independent of ϵ, it is necessary that

$$\mu_1^* = \ln \frac{\rho}{\tilde{\rho}_{\text{op}}} \tag{5.9}$$

and, hence,

$$\mu_2^* = \frac{1}{2} \ln \frac{\tilde{\rho}^{(2)}}{\tilde{\rho}_{\text{op}}^{(2)}}. \tag{5.10}$$

These are the same as the expressions obtained applying virtual exchange to each reservoir independently. Thus, we can understand the value given by Eq. (5.10) as $\overline{\mu_2^*}$. Figure 17 shows $|\mu_1^* - \mu_2^*|$ as a function of density computed via virtual exchange directly in fixed-N simulations for system sizes $L = 10, 20, 28, 56, 64, 96,$ and 128. The left panel corresponds to equilibrium ($D = 0$) and the right to $D = 1$. The lower graphs in each column show detailed plots of $|\mu_1^* - \mu_2^*|$ in

the range of densities for which nonequilibrium effects are strongest. As L increases, the difference between the two chemical potentials vanishes in equilibrium, while for $D = 1$ it converges to a well defined nonzero value.

C. Discussion

To understand why the coexistence value of μ^* depends on the exchange scheme ζ when $\mathcal{S}$ is out of equilibrium, we recall the definition of particle current, Eq. (3.2). One can rearrange this expression to yield

$$J_N^\zeta(\mu^*) = \frac{|\Delta N|}{2} \sum_{\mathcal{C},\mathcal{C}'} [w(\mathcal{C}'|\mathcal{C})\tilde{p}_\mathcal{C} - w(\mathcal{C}|\mathcal{C}')\tilde{p}_{\mathcal{C}'}]. \quad (5.11)$$

It is clear that if $\tilde{p}_\mathcal{C} = p_\mathcal{C}^{\mathrm{eq}}$ $(D = 0)$, the current is zero, independent of ζ, because microscopic detailed balance holds, guaranteeing that each contribution to the particle current due to insertion is compensated by removal. Out of equilibrium, however, microscopic detailed balance no longer holds, and zero particle current is the net result of many contributions which individually are unbalanced. Thus there is no reason to expect Eq. (3.10) to hold for arbitrary ζ, and the choice of the exchange scheme determines the value of μ_ζ^*; the schemes employed here for $\mathcal{R}_1$ and $\mathcal{R}_2$ provide an example. Nevertheless, if $\tilde{p}_\mathcal{C} = p_\mathcal{C}^{\mathrm{eq}}$, as is true for certain nonequilibrium models (e.g., the zero range process [14]), reservoir independence should hold.

VI. CONCLUSIONS

We investigate an aspect of the definition of an effective chemical potential μ^* for NESS that has been overlooked until now. Starting from the concept of coexistence, we define a fixed-μ^* description for a stochastic lattice gas with NNE, a simple model with nontrivial NESS properties. We ask whether the two thermodynamic descriptions, one with fixed particle number [fixed-$(N, V; D|\zeta_1, 0)$], the other with fluctuating particle number [fixed-$(\mu^*, V; D|\zeta_1, \epsilon \to 0)$], are equivalent in the TL. We find the two descriptions to be equivalent at three levels: macroscopic, thermodynamic, and in distribution. A important consequence is that the probability density of the (particle) density can be described in terms of a large-deviation function.

In addition, we show that in the fluctuating particle number framework, two particle reservoirs with distinct mechanisms of particle exchange (ζ) lead to distinct values of the intensive parameter. Thus, reservoir independence does not hold out of equilibrium. The value of μ^* attributed to a NESS depends on how it exchanges particles with the reservoir. This makes it possible for a driven system to transfer particles from a reservoir at a chemical potential to another at a higher chemical potential.

Since this paper is part of an attempt to define intensive parameters for NESS via coexistence with a reservoir, dependence of μ^* on the exchange mechanism is an unwelcome complication. The fundamental criterion of consistency (i.e., the zeroth law) can only be expected to hold for each *specific exchange scheme*, not for all simultaneously. It is nevertheless possible to establish equivalences between two distinct exchange mechanisms using the properties of fixed-N systems, as shown here using results from fixed-particle-number simulations. Thus, intensive parameters defined via coexistence *retain their predictive power*.

Although our results are obtained for a specific system (the NNE lattice gas), we expect them to hold for other models in NESS. An interesting example for future study is the KLS-driven lattice gas [11], since it possesses two intensive parameters, effective chemical potential and temperature. In the KLS model, the relation between macrostate and thermodynamic equivalence still holds. We believe that the probability distribution over the number of particles will satisfy a large deviation principle in the TL, since the macroscopic particle removal rate is a monotocically increasing function of density and the particle insertion rate is monotonically decreasing function of density.

Description equivalence appears to be a general property of stochastic particle processes with reflecting barriers at $N = 0$ and $N = N_{\mathrm{max}}$. For nonathermal systems such as the KLS model, one may also ask whether the fixed- and variable-*energy* descriptions are equivalent in the thermodynamics limit. Since the stationary distribution (of energy) under stochastic energy exchange is again characterized by a vanishing probability current, it seems reasonable to expect that description equivalence will hold in this case as well.

We intend to address these questions in future work. Finally, a further challenge is the definition of intensive parameters for systems in contact with reservoirs away from the weak-exchange-limit. We believe that understanding coexistence away from the WEL may hold the key to a problem that has resisted analysis until now: How to predict the density profile in nonuniform NESS involving walls or a spatially varying drive.

[1] Y. Oono and M. Paniconi, Steady state thermodynamics, Prog. Theor. Phys. Suppl. **130**, 29 (1998).

[2] S. Sasa and H. Tasaki, Steady state thermodynamics, J. Stat. Phys. **125**, 125 (2006).

[3] R. Dickman and R. Motai, Inconsistencies in steady-state thermodynamics, Phys. Rev. E **89**, 032134 (2014).

[4] J. Guioth and E. Bertin, Large deviations and chemical potential in bulk-driven systems in contact, Europhys. Lett. **123**, 10002 (2018).

[5] J. Guioth and E. Bertin, Nonequilibrium chemical potentials of steady-state lattice gas models in contact: A large-deviation approach, Phys. Rev. E **100**, 052125 (2019).

[6] E. Bertin, K. Martens, O. Dauchot, and M. Droz, Intensive thermodynamic parameters in nonequilibrium systems, Phys. Rev. E **75**, 031120 (2007).

[7] P. Pradhan, R. Ramsperger, and U. Seifert, Approximate thermodynamic structure for driven lattice gases in contact, Phys. Rev. E **84**, 041104 (2011).

[8] L. Ferreira Calazans and R. Dickman, Steady-state entropy: A proposal based on thermodynamic integration, Phys. Rev. E **99**, 032137 (2019).

[9] R. Dickman, Failure of steady-state thermodynamics in nonuniform driven lattice gases, Phys. Rev. E **90**, 062123 (2014).

[10] R. Dickman, Phase coexistence far from equilibrium, New J. Phys. **18**, 043034 (2016).

[11] S. Katz, J. L. Lebowitz, and H. Spohn, Phase transitions in stationary nonequilibrium states of model lattice systems, Phys. Rev. B **28**, 1655 (1983).

[12] S. Chatterjee, P. Pradhan, and P. K. Mohanty, Zeroth law and nonequilibrium thermodynamics for steady states in contact, Phys. Rev. E **91**, 062136 (2015).

[13] H. Touchette, Equivalence and nonequivalence of ensembles: Thermodynamic, macrostate, and measure levels, J. Stat. Phys. **159**, 987 (2015).

[14] M. R. Evans and T. Hanney, Nonequilibrium statistical mechanics of the zero-range process and related models, J. Phys. A: Math. Gen. **38**, R195 (2005).

[15] Jules Guioth and Eric Bertin, Nonequilibrium grand-canonical ensemble built from a physical particle reservoir, Phys. Rev. E **103**, 022107 (2021).

[16] The NNE model exhibits an order-disorder phase transition [17]. In equilibrium, it can be understood as a entropically driven phase transition; the critical density is $\rho_c = 0.3677429990410(3)$ [18]. Out of equilibrium, for NNE with hopping to first and second neighbors, for maximum drive ($D = 1$), the phase transition occurs at density $\rho_c \approx 0.350(5)$ [19]. The trasition belongs to the Ising universality class in both cases.

[17] R. Dickman, First- and second-order phase transitions in a driven lattice gas with nearest-neighbor exclusion, Phys. Rev. E **64**, 016124 (2001).

[18] W. Guo and H. W. J. Blöte, Finite-size analysis of the hard-square lattice gas, Phys. Rev. E **66**, 046140 (2002).

[19] A. Szolnoki and G. Szabó, Influence of extended dynamics on phase transitions in a driven lattice gas, Phys. Rev. E **65**, 047101 (2002).

[20] For finite systems, the stationary distribution starting from a nonjammed initial configuration is unique. By a jammed configuration, we mean one in which some or all particles are prohibited from moving. We restrict our analysis to the nonjammed subspace.

[21] B. Widom, Some topics in the theory of fluids, J. Chem. Phys. **39**, 2808 (1963).

[22] H. Touchette, The large deviation approach to statistical mechanics, Phys. Rep. **478**, 1 (2009).

[23] D. Ruelle, *Statistical Mechanics: Rigorous Results* (W. A. Benjamin, Amsterdam, Netherlands, 1969).

[24] R. Dickman, Numerical analysis of the master equation, Phys. Rev. E **65**, 047701 (2002).